Thermochimica Acta 664 (2018) 73–80

Contents lists available at ScienceDirect

Thermochimica Acta

journal homepage: www.elsevier.com/locate/tca

Enhanced CO_2 capture capacity on open-cell Mg foams via humid impregnation with lithium at low temperatures

M. Velasco-Castro, I.A. Figueroa*, H. Pfeiffer, J.F. Gómez-García

Instituto de Investigaciones en Materiales, Universidad Nacional Autónoma de México (UNAM), Circuito Exterior S/N, Cd. Universitaria, C.P. 04510, Mexico City, Mexico

ARTICLE INFO

Keywords:
Magnesium foams
Lithium
Oxidation
CO_2 capture
Thermogravimetric analysis

ABSTRACT

In the present work, carbon dioxide capture capacity was evaluated after a humid impregnation process performed on the surface of open-cell magnesium (Mg) foams, with an alkaline solution of lithium hydroxide (LiOH). The Mg foams were fabricated by the infiltration casting method, using irregular particles of sodium chloride (NaCl) as space holders. Optical microscopy, helium (He) pycnometry and nitrogen (N_2) adsorption-desorption techniques were used to measure the pore size, density (ρ_{foam}) and specific surface area (A_s), respectively. The microstructural modifications after the impregnation process were analysed by means of X-ray diffraction (XRD) and scanning electron microscopy (SEM). Afterwards, a thermogravimetric analysis was performed to evaluate the CO_2 capture capacity under different water steam (H_2O) conditions. After the H_2O–CO_2 chemisorption process, the carbonated products were identified by the attenuated total reflexion – Fourier transform infrared spectroscopy (ATR-FTIR) technique and then, quantified through a thermal decomposition process. Thermal analysis outcomes showed that H_2O–CO_2 chemisorption capacity of the Mg foams considerably increased after lithium (Li) impregnation. The later as consequence of the lithium oxide (Li_2O) high reactivity with CO_2, and its effect on the thickening of the oxide film layer formed on the surface of the open-cell Mg foams. These results promote the possible use of this kind of cellular material as structured CO_2 captor, proposing a new functional application for metallic foams and giving an alternative solution to the current environmental issues.

1. Introduction

Cellular metals and metallic foams have been used in a number of structural and functional applications [1–5], such as fluid filters, heat exchangers, supports for catalysis and most recently as structured carbon dioxide (CO_2) captors [6]. Because of porosity, these materials have shown an excellent combination in their physical and mechanical properties, for instance, high energy-impact absorption accompanied by a relative low-mass or mainly due to high-strength to light-weight ratio, among other features [1,5]. Recently, Mg foams have not only demonstrated capabilities for several functional purposes like thermal and acoustic insulation [3,4], but also as a promising biomaterial for bone implants [7,8]. However, environmental functions have not been deeply studied. From engineering and ecological points of view, open-cell Mg foams are able of preserving both, functional and structural applications, meanwhile they can also be used as structured CO_2 captors. It has been proved that these type of materials can be successfully applied in the chemisorption of CO_2 [6].

Nowadays, efforts to face up and diminish the current effects of environmental issues related to global warming, have become an imperative global concern [9], and both theoretical and practical research are, constantly, being developed [10–16]. Within all carbon capture and storage technologies, many sorbent materials, i.e. activated carbons, zeolites, organic-inorganic hybrids, hydrotalcite-like compounds, alkali-metal ceramics and calcium oxide, have been mainly studied and proposed as prominent CO_2 captors [10,12,13]. Nevertheless, alkali-metal-based oxides have attracted great interest as a result of their high-adsorption capacity, low-cost and availability [11,14]. Recently, several manuscripts have reported the capture of CO_2 by applying binary compounds of metallic oxides, with at least one alkali-metal in their chemical composition, in a wide range of temperatures [11,14]. Moreover, owing to catalytic activity offered by these type of materials, their application has not been exclusively limited to separate CO_2 from pre-combustion or post-combustion flue gases, but also to perform steam reforming processes, such as CH_4 or CO conversion to CO_2 [17].

It has been reported that chemical and physical modifications performed on different ceramic materials with lithium (Li), either doped or mixed to produce solid solutions, enhance the kinetic factors, promoting a greater chemisorption capacity of CO_2 [18]. It is worthy of

* Corresponding author.
E-mail address: iafigueroa@unam.mx (I.A. Figueroa).

https://doi.org/10.1016/j.tca.2018.04.009
Received 21 February 2018; Received in revised form 17 April 2018; Accepted 18 April 2018
Available online 30 April 2018

note that these modifications could reach a high amount of CO_2 capture under dry conditions [19]. On the other hand, several ceramics compounds such as aluminates ($\alpha - Li_5AlO_4$) [20], cuprates (Li_2CuO_2) [21], ferrites ($Li_{1+x}FeO_2$) [22], silicates (Li_8SiO_6) (Li_4SiO_4) [23] and zirconates (Li_2ZrO_3) [24], have been tested under water steam flows and low temperatures (30–80 °C), showing promising results for CO_2 capture. Likewise, it is also reported that addition of alkali-metals (e.g. Li, Na and K) via humid impregnation on different adsorbent materials, such as hydrotalcite-like compounds [25,26] or metallic oxides [27], notably modified their textural properties (e.g. surface area, porosity, particle size, etc.) and therefore, their CO_2 chemical sorption capacities are also influenced and indeed improved.

The key advantages offered by open-cell Mg foams are their excellent mechanical properties, high surface area and interconnected porosity. The latter implies more active surface available for chemical reactions, allowing gases to flow freely throughout the entire porous network. Moreover, these materials might be used in several cycles after a decarbonation process. Hence, the objective of the present work was to study the CO_2 capture capacity on open-cell Mg foams after being impregnated with lithium via humid media (alkaline solution) and subsequently oxidized under certain conditions. The process of CO_2 capture was carried out under different humid conditions and low temperatures.

2. Experimental procedure

2.1. Fabrication of open-cell Mg foams

Open-cell Mg foams were manufactured by the infiltration casting method. This method has been widely applied to produce cellular materials with complete open-porosity [4,8]. Argon (Ar, 99.99%) was used to maintain an inert atmosphere, promoting the infiltration of the molten metal throughout the irregular particles of sodium chloride (NaCl, 99.95%). NaCl particles were sieved and classified in one average size (510–710 μm). Firstly, NaCl particles were deposited inside the crucible to assemble the porous preform, and then Mg ingots (99.5%) were located on top of them. The dimensions of the austenitic stainless-steel 304 cylindrical-chamber are 73 mm of outer diameter, wall thickness of 2.9 mm and a height of 20 cm. Thereafter, the casting process takes place and the Mg load was melted at 750 °C under a constant gas pressure of 50 kPa, for 1 h. Afterwards, the molten metal was infiltrated through the preform using a gas pressure of 1.5 bar for 15 min, and subsequently cooled down at room temperature. After this, a complete solid Mg–NaCl composite was produced, and then the final ingot was machined to obtain several cubic-shaped samples ($\sim 1 cm^3$) for the study. With the aim of removing the NaCl particles and obtaining a free-salt metallic foam, the Pourbaix diagram (potential − pH) was considered [28]. Hence, the composite was immersed into an alkaline solution of sodium hydroxide (NaOH, 99.95%, pH = 13) to dissolve the NaCl particles and prevent corrosion by pitting [28]. Because of the pores and dimensions of the cubic-shaped samples (with shallow relative depth), the implementation of ultrasonic vibrations was enough to increase the dissolution rate and release gas bubbles entrapped into the porous network, avoiding overexposure to the alkaline solution that might lead to detrimental effects, such as corrosion.

From the micrographs obtained by optical microscopy, at least 100 measurements were taken to estimate the average pore size. The last mentioned was achieved by using an image processing software and the line intercept sampling. An Ultrapyc-1200e pycnometer for solids (pulse method and helium atmosphere) was used to determine the density of the open-cell Mg foams (ρ_{Mg}), and subsequently the percentage of porosity (% Pr) was calculated by means of the relative density ($\rho_{Relative}$). BET specific surface area was determined by N_2 adsorption-desorption experiments, which were performed on a Bel-Japan Minisorp II equipment at 77 K using a multipoint technique. The samples were degasified at 80 °C for 24 h under vacuum, prior to the corresponding analysis.

2.2. Impregnation and superficial oxidation of the open-cell Mg foams

An alkaline solution of lithium hydroxide (LiOH) with pH = 13 was prepared. This solution was used as lithium-ion precursor, and to prevent possible corrosion effects on the surface as already explained. The cubic-shaped samples were immersed into the LiOH solution for 30 min. Then, the impregnated samples were dried off, by a superficial oxidation process, in a tubular furnace using an oxygen (O_2, 99.99%) flow of 40 mL/min at 500 °C for 1 h. With the aim of conserving the structural integrity of an open-cell Mg foam, a thin oxide layer must be formed after the superficial oxidation process. Therefore, these experimental conditions (500 °C for 1 h) were previously established to form an oxide layer of 6 (±2) microns on the cell walls of an open-cell Mg foam [6].

With the aim of identifying the crystal phases formed during the oxidation stage, and after the CO_2 capture process; oxidized samples and carbonated products were characterized by X-ray diffraction (XRD), using a diffractometer Bruker AXS-D8 Advance, coupled to a copper (Cu) anode X-ray tube ($\lambda_{Cu-K\alpha_1} = 0.15406nm$) working at 30 kV and 30 mA, with a step size of 0.02° (2θ) and step time of 12 s in the range from 30° to 80°. X-ray patterns were identified by the corresponding Joint Committee Powder Diffraction Standards (JCPDS) files. Furthermore, the microstructural morphology of the samples before and after the CO_2 capture process was analysed with a scanning electron microscope JEOL JMS-7600F. Additionally, all samples, before and after the CO_2 capture process, were analysed by Fourier transform infrared (FTIR) spectroscopy using the attenuated total reflexion (ATR) module on a spectrometer Alpha-Platinum (Bruker).

2.3. CO_2 capture experiments

Dynamic and isothermal experiments were performed using a humidity-controlled thermo-balance TA instrument model Q5000SA. Experiments were carried out using distilled water, and CO_2 (Praxair, grade 3.0) as carrier gas with a flow rate of 60 mL/min. Dynamic H_2O–CO_2 sorption-desorption isothermal experiments were performed at different temperatures (40 and 60 °C) while varying the relative humidity (RH) from 0 to 80% and then from 80 to 0% at a rate of 0.5% per minute. On the other hand, isothermal measurements were performed at specific temperatures (40 and 60 °C) and different values of RH (30, 50 and 70%) for each temperature condition. Thereafter, XRD, SEM, and FTIR techniques were used to characterize the samples and identify the carbonated products. With the aim of quantifying the amount of H_2O–CO_2 sorbed on the surface, a thermogravimetric analysis (TGA) was performed under nitrogen (N_2, Praxair grade 4.8) atmosphere, using a thermo-balance TA instrument model SDT600. The decomposition process was carried out within a temperature range of 30–450 °C, with a heating rate of 5 °C per minute.

3. Results and discussion

3.1. Porous structure

Fig. 1 shows the micrograph that corresponds to the cellular network of an open-cell Mg foam manufactured by the infiltration casting method with an average pore size of 710 ± 30 μm (μm), using irregular particles of NaCl as space holders. From this image, a uniform pore distribution and complete interconnected porosity are corroborated through the whole volume of the structured material. Moreover, regarding the size and shape of the porous network, both aspects are equivalent to those particles used as space holders. As mentioned before, these features are appropriate for the objectives of the present work, since gases will be allowed to flow freely throughout the entire porous network. On continuing the structural-physical analysis, the relative density ($\rho_{Relative}$) was determined with the following expression:

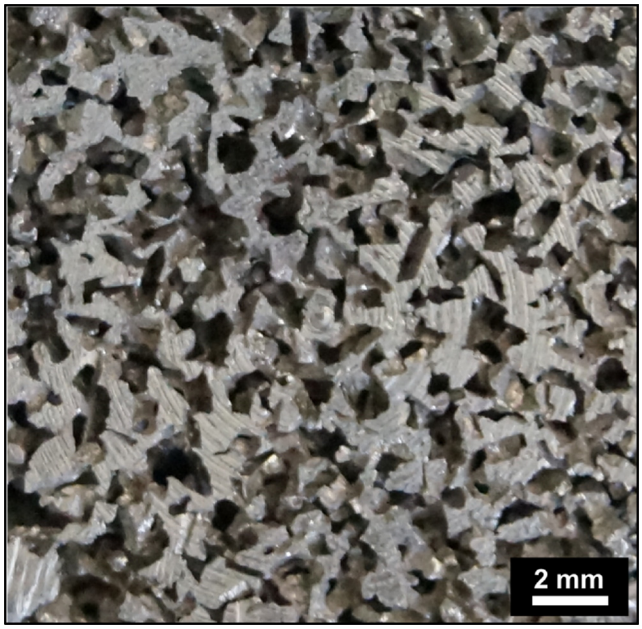

Fig. 1. Cell structure of an open cell Mg foam, manufactured by the infiltration casting method.

$$\rho_{Relative} = \frac{\rho_{foam}}{\rho_{Mg}} \quad (1)$$

According to the aforementioned, the open-cell Mg foam density (ρ_{foam}) was measured. The metal matrix density was considered as 1.74 g/cm^3 [29]. Subsequently, the percentage of porosity (% Pr) was calculated with the well-established expression for materials with an open-cellular structure [1]:

$$\%Pr = (1 - \rho_{Relative}) \times 100 \quad (2)$$

The outcomes measured by means of optical microscopy and helium (He) pycnometry were the following: pore size of 710 ± 30, ρ_{foam} = 0.54g/cm^3, $\rho_{Relative}$ = 0.31 and %Pr = 69%.

3.2. Characterization of the modified surface with Li

3.2.1. X-ray diffraction

Fig. 2 displays the XRD patterns that correspond to an open-cell Mg foam whose surface has been modified with Li (after being immersed into the ion precursor solution, and subsequently oxidized). Additionally, it also shows the corresponding pattern of a sample that was not impregnated, but oxidized at 500 °C for 1 h. From the diffractogram, the identified reflections corresponded to the Mg (JCPDS 00-004-0770), MgO (JCPDS 01-089-4248) (Periclase) and Li_2CO_3 (00-022-1141) (Zabuyelite) crystalline phases. Moreover, it can be observed that Mg was the dominant phase of the modified surface.

The appearance of a lithium carbonate (Li_2CO_3) reflection may suggest the previous formation of lithium oxide (Li_2O). As a result of Li_2O high reactivity with CO_2, Li_2O suffers an spontaneous carbonation process, even at normal conditions (room temperature and air atmosphere), as previously reported [30]. These results agree well with those XRD patterns reported in references [31,32], where Li/MgO catalysts were synthetized via sol-gel method, and wet impregnation. In these reports, the detection of MgO and Li_2CO_3 reflections, for both ways of synthesis, was mentioned. The absence of any other phase related to Li, including the $LiNO_3$ chemical compound precursor and the Li_2O high chemical affinity with CO_2 were also emphasized.

On the other hand, some notorious differences between the XRD patterns of unmodified and modified open-cell Mg foams were clearly observed. These differences confirmed that the microstructural changes

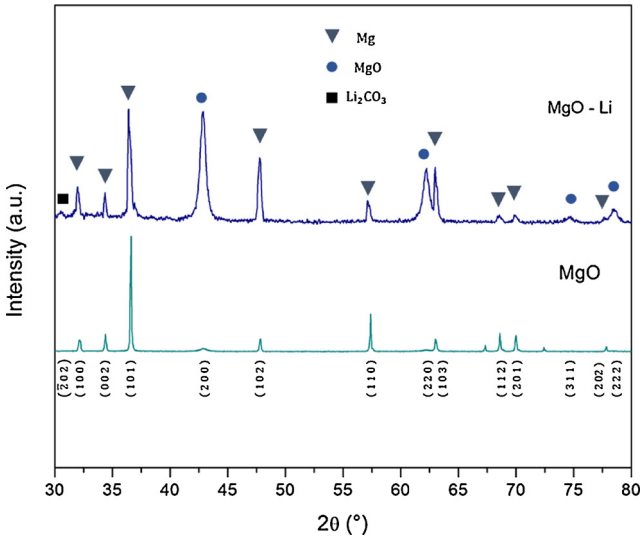

Fig. 2. X-ray diffraction patterns of an open-cell Mg foam after being impregnated with Li and one which corresponds to an unmodified open-cell Mg foam, both oxidized at 500 °C for 1 h.

on the modified surface are rather important. The first aspect to note is that MgO width peaks were modified, indicating that the crystallite size (D) increased from 12.3 to 15 nm. These measurements were estimated using Scherrer equation (3). The values of the FWHM (full width at half-maximum) and θ were calculated by a Pseudo-Voight function. The Scherrer factor (shape factor, k) was considered as 0.9, and the wavelength (λ_{Cu}) as 0.15406 nm. The reflection (200) that corresponds to the MgO was selected as reference. The selection criteria were based on its position, intensity, sharpness and absence of peak overlap [33].

$$D = \frac{k \cdot \lambda_{Cu}}{FWHM \cdot \cos\theta} \quad (3)$$

The second aspect was related to the increment of MgO peaks intensities after the impregnation process. A plausible explanation of such intensity increments could be attributed to the thickening of MgO layer, as the reflections kept the same height intensity ratio, therefore discarding any possible effect of preferential orientation due to the manufacturing process or sample's position in the X-ray diffraction equipment. Furthermore, it is well known that magnesium and its different alloys are prone to react at normal conditions. Hence, an oxide film can be spontaneously formed on their surface. A great number of studies have focused on the chemical and physical stability of such oxidized layer [34–36]. In the literature, it has been reported the effect of lithium as an alloying element, where the oxide film on a Mg–Li cast alloy, is thicker than on the pure Mg. The latter as a result of Li and its more susceptible oxidizing behaviour [37]. Hence, the effect of Li on the oxide layer formation and the thickening of the MgO layer, can be explained in terms of the aforementioned.

3.2.2. Scanning electron microscopy and nitrogen adsorption-desorption isotherm

Fig. 3a displays the micrograph corresponding to the surface of the sample, impregnated with Li, after being oxidized. Fig. 3b shows the N_2 adsorption-desorption curves for modified and unmodified surface samples. From Fig. 3a, a uniformly distributed rough morphology can be observed over the entire surface. In addition, due to the brittle nature of oxides, the oxidized surface contains some micro-cracks and some material fragmentation that might reduce its adherence to the Mg matrix. These defects agree with the Pilling/Bedworth ratio of the Li_2O (P/ B= 0.58), which means that lithium oxides cannot form a compact oxide layer.

Regarding the N_2 adsorption-desorption isothermal experiments,

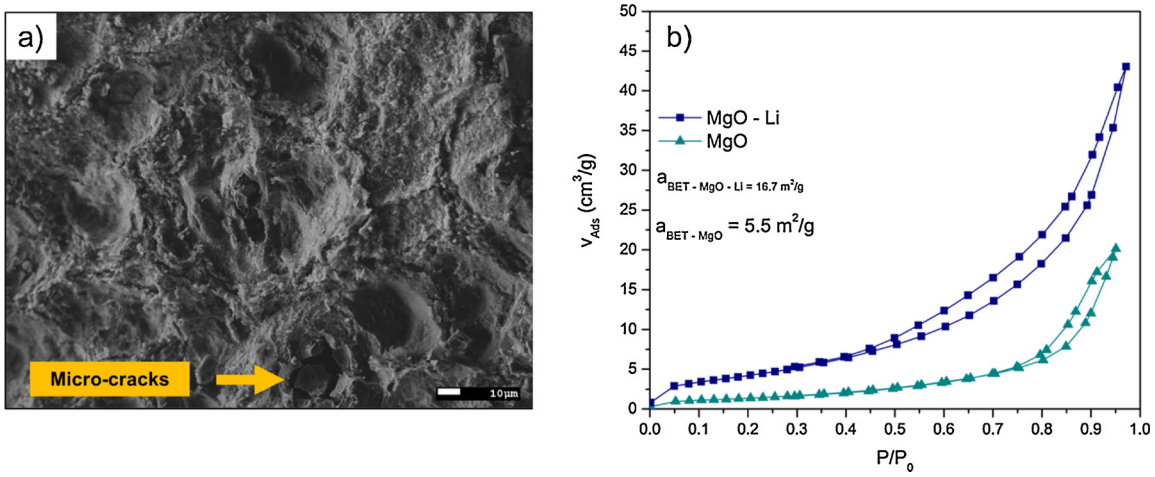

Fig. 3. Secondary-electron micrograph of the modified surface (left). N_2 adsorption-desorption curves (right).

both samples presented type IV isotherms according to IUPAC classification, which is characteristic of mesoporous materials with low energy adsorption [38,39]. However, the porosity of open-cell Mg foams (pore size of 710 ± 30 µm) is very far from being considered into this classification, since the diameter of the mesopore ranges from 2 to 50 nanometres (nm) [38,39]. Consequently, the hysteresis loops, generally related to mesoporosity, are attributed to the composition and structural modifications performed on the oxidized layer, after impregnation with Li.

There is a notorious difference between the hysteresis loops for the MgO–Li and MgO samples. The loop for MgO–Li showed a higher adsorbed volume, and consequently the degasification process time took much longer. This phenomenon was attributed to the specific surface area, which was enlarged after the addition of Li, reaching 16.7 m^2/g. However, it should be mentioned that the specific surface area, obtained by open-cell Mg foams impregnated with Li, can achieve similar results to those reported by powder based materials without mesoporosity, 0.5 m^2/g [40] and 3.6 m^2/g [41].

3.3. CO_2 capture at low temperatures

3.3.1. Dynamic isothermal experiments

Fig. 4 shows the dynamic sorption-desorption H_2O–CO_2 isothermal experiments performed on the modified surface with Li and the corresponding to an unmodified sample at low temperatures (40 and 60 °C) while varying the RH from 0 to 80% (sorption) and then from 80 to 0% (desorption).

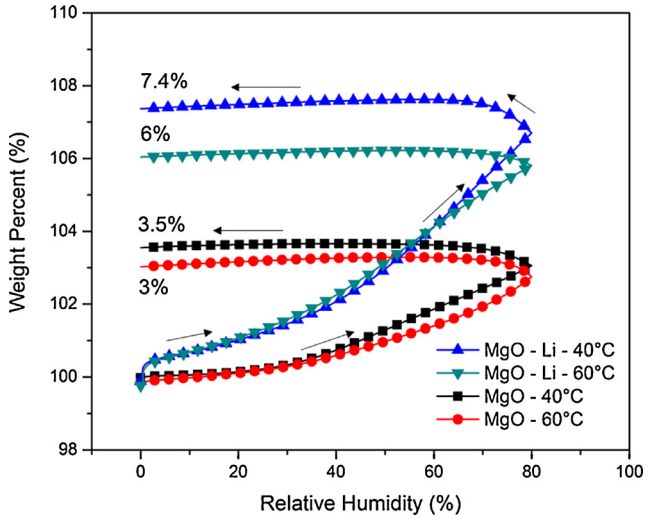

Fig. 4. Dynamic adsorption-desorption H_2O–CO_2 isothermal curves under a wide range of RH.

Fig. 4 shows that all isotherms displayed a non-closed hysteresis loop. This behaviour was attributed to the hydration, hydroxylation and carbonation reactions processes on the modified surface. Considering that the carbonation process of MgO under the presence of water vapour has been deeply studied, it has been proved that MgO can sorb water at low temperatures (40–70 °C) and with different humidity conditions, using N_2 as carrier gas. In addition, the carbonation process ($MgCO_3$) was also reported after switching N_2 for CO_2 [42]. Therefore, the reported in ref [42] agrees well with the results obtained in this work by means of dynamic isothermal experiments, performed on both samples (MgO–Li and MgO) (Fig. 4). These results corroborated that relative humidity tended to increase the H_2O–CO_2 capture capacity on MgO. Bearing in mind that as the temperature decreases, the evaporation rate drops, enhancing the H_2O–CO_2 capture capacity. The following reaction mechanism for the MgO–H_2O–CO_2 system has been reported [43]:

$$Mg_{(s)} + \frac{1}{2}O_{2(g)} \rightarrow MgO_{(s)} \quad \text{(R1)}$$

$$MgO_{(s)} + H_2O_{(v)} \rightarrow Mg(OH)_{2(s)} \quad \text{(R2)}$$

$$Mg(OH)_{2(s)} + CO_{2(g)} \rightarrow MgCO_{3(s)} + H_2O_{(v)} \quad \text{(R3)}$$

On the other hand, the effect of Li on the surface of an open-cell Mg foam was positive during the H_2O–CO_2 chemisorption process. Indeed, a slightly higher kinetic behaviour at the beginning of the isotherms for both temperatures (40 and 60 °C) was clearly observed. Regarding the mechanism for the H_2O–CO_2 capture reactions on the modified surface, it has been reported the chemisorption process of CO_2 on LiOH as an intermediate reaction [21]. In the literature, it has been reported that Li_2O may moderately capture CO_2 (~14.3%) within temperatures ranging from 190 to 400 °C, under dry conditions [30]. Hence, it can be argued that water vapour should act as intermediate chemical specie within the current system, modifying the activation energy of the whole chemisorption process of CO_2 on Li_2O.

3.3.2. Kinetic isothermal experiments

The kinetic isothermal experiments were performed on the modified surface at low temperatures (40 and 60 °C) and different RH conditions (30, 50 and 70%). The kinetic isothermal curves are shown in Fig. 5. From these figures, it can be seen that H_2O–CO_2 capture capacity increased as a function of RH. However, at 40 and 7% RH, the isotherm showed an atypical behaviour. Form the plot of Fig. 5a, it is seen that the CO_2 capture percentage is higher for the sample treated at 50 RH

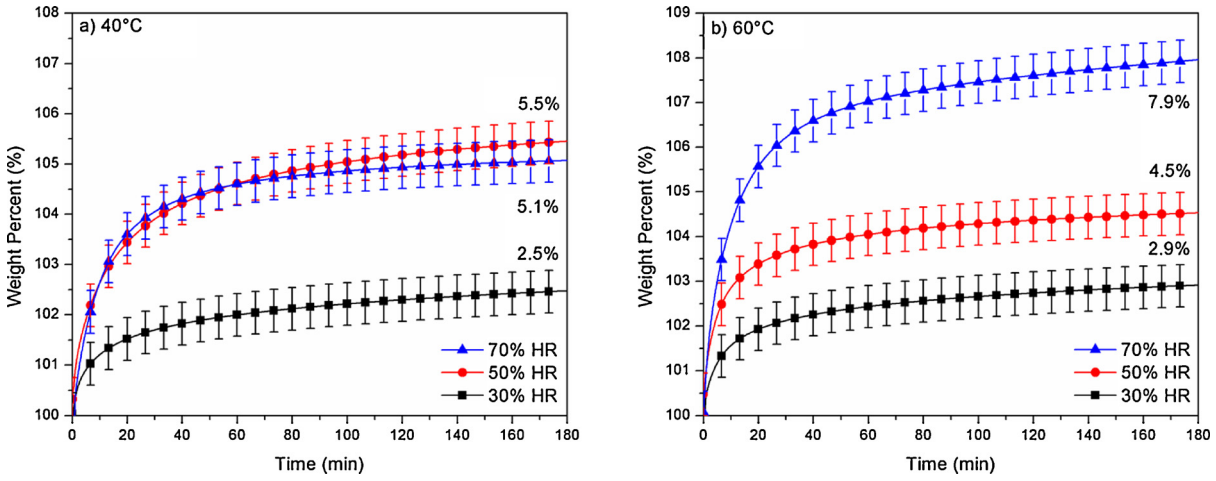

Fig. 5. Kinetic H_2O–CO_2 isothermal experiments performed on samples with modified surface at low temperatures (40 and 50 °C) and different RH conditions.

than that for the 70 RH.

A plausible explanation to this phenomenon can be attributed to the saturation between the solid-gas interface, where the water vapour could be wetting the sample surface, blocking the interactions between the formed hydroxides and CO_2. The samples treated at 60 °C–70% RH and 40 °C–50% RH presented the highest weight increment, 7.9% and 5.5%, respectively. Hence, the H_2O–CO_2 capture capacity was also increased as function of temperature, which should thermodynamically promote the formation of $MgCO_3$ and Li_2CO_3. It is worth to mention that the chemisorption capacity and kinetic were considerably enhanced when compared to those reported previously (open-cell Mg foams without modified surface) [6]. This CO_2 capture improvement was the consequence of the Li addition and its high affinity to CO_2.

3.4. Characterization and identification of products

3.4.1. X-ray diffraction

Fig. 6 illustrates the XRD patterns that correspond to the samples that reached the highest H_2O–CO_2 chemisorption capacity after the kinetic isothermal experiments. From this figure, it can be noticed the absence of carbonated species reflections. This is attributed to their concentration, which must be out of the limit detection offered by the XRD technique. Nevertheless, considering that MgO peak intensities kept the same height ratio, it can be argued that the intensity reduction on the MgO reflection (200) could be attributed to a drop of MgO concentration and therefore, may suggest a carbonation process.

3.4.2. Scanning electron microscopy

A micrograph of the surface after being treated at 60 °C–70% RH (kinetic isothermal experiment with the highest weight gained) is displayed in Fig. 7. In the micrograph, a completely modified morphology can be seen, in comparison to that of Fig. 3 (after being impregnated and oxidized). This difference could be explained in terms of the new chemical species formed on the surface. In addition, the presence of some defects such as micro-cracks were clearly observed. These cracks are attributed to the sample volume change, supporting the formation of highly fragile species.

As it is known, lithium quantification is not possible by Energy-Dispersive Spectroscopy (EDS) micro-analysis. However, this was performed to compare the atomic percent values for oxygen (O), carbon (C) and magnesium (Mg) elements, before and after the kinetic isothermal experiments. Such values were useful to verify, indirectly, the formation of carbonated species. Besides, it is worth mentioning that the values obtained by this analysis were normalized as function of the identified elements. Table 1 shows the results of the elemental micro-analysis.

The results obtained for the modified surface (after impregnation process) suggested the formation of MgO, since the EDS results for Mg

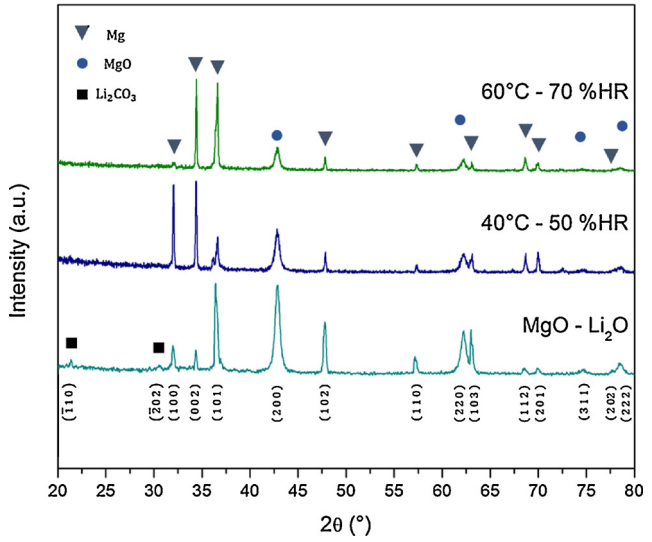

Fig. 6. XRD patterns for open-cell Mg foams with modified surface and samples isothermally treated at specific conditions.

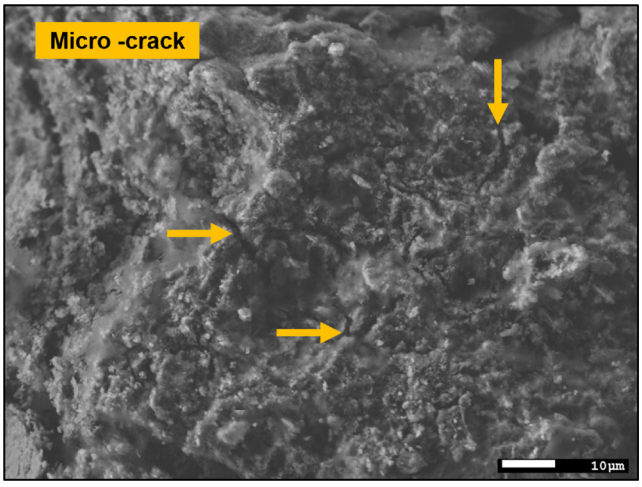

Fig. 7. Micrograph corresponding to the sample with modified surface after being treated at 60 °C–70% RH.

Table 1
Elemental analysis by EDS on the modified surface before kinetic experiment and after being treated at 60 °C–70% RH.

	Atomic Percent (%)	
Element	Modified surface	Treated at 60 °C–70% RH
Mg	47.51	28.11
O	44.01	57.96
C	8.47	13.93

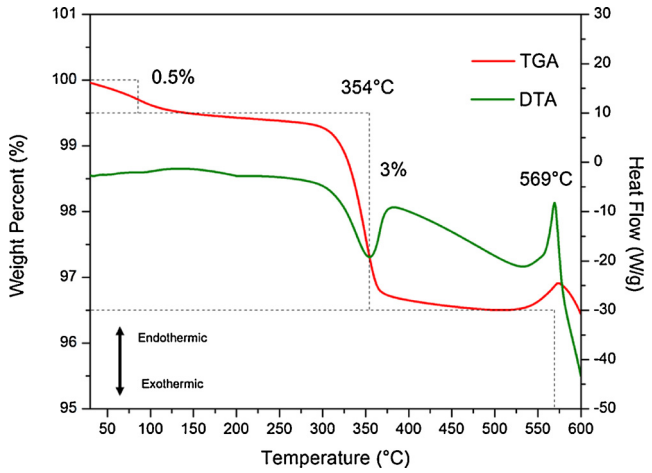

Fig. 8. TGA-DTA curves for a sample with carbonated surface (with modified surface).

and O are close to the stoichiometric composition of MgO. In addition, the atomic percent value for C in the same column (modified surface) may confirm the previous formation of carbonated species such as Li_2CO_3 that was previously identified by means of XRD (Fig. 2). Besides, it is evident that numeric variations between Mg, O and C for the sample treated at 60 °C–70% RH, cannot be completely attributed to the $MgCO_3$. Moreover, such numbers were far from being comparable to the $MgCO_3$ stoichiometry. Nevertheless, a possible effect of the carbonated species associated to Li located on the surface could also be considered.

3.4.3. Fourier transform infrared spectroscopy

As it was not possible to identify the carbonated products by means of XRD, the FTIR technique was carried out to identify the chemical species formed on the modified surface. Only samples with the highest weight increment after kinetic isothermal experiments (40 °C–50% RH and 60 °C–70% RH) were considered. Subsequently, the same samples but after being decomposed by means of thermogravimetric analysis, were also analysed. It is worth to mention that the decomposition process was performed within a temperature range from 25 to 450 °C. The melting point of Li_2CO_3 (710 °C) was considered [30]. The operating range was established as function of Mg melting point (650 °C) [29]. To justify such conditions, a TGA-DTA was carried out on a carbonated sample (with modified surface). Fig. 8 shows the TGA and DTA curves. From the thermogram, a dehydration process (first drop in weight) is observed between room temperature and 200 °C. One of the first things to note is an exothermic reaction at 354 °C, which is attributed to thermal decomposition of carbonated species. It is worth mentioning that a dehydroxylation process is no considered, since no signals of H_2O or O–H were identified in further results (FTIR analysis). Then, an endothermic event occurs at 569 °C that corresponds to the casting of Mg metal matrix. These results are important, since there is not a noticeable weight loss between 450 and 550 °C (before casting temperature) that could be attributed to the decomposition of secondary phases or weak adsorbed species, such as carbonates. Therefore, this justifies the selected range of temperatures (25–450 °C) to perform the analysis.

On continuing the FTIR analysis, Fig. 9 shows the IR spectra obtained from the samples that achieved the highest weight increment (40 °C–50% RH and 60 °C–70% RH) after kinetic isothermal experiments. In addition, spectra before such experiments (samples with modified surface) and after being thermally decomposed were also considered. From both IR spectra, it can be seen the signal or band vibration at 1421 cm^{-1} that corresponds to the carbonate ion (CO_3^{-2}) [44,45]. However, no signals of H_2O or O–H species were identified. A first point that clearly stands out is that samples with modified surface (MgO – Li) presented the same band vibration at 1421 cm^{-1}, which corroborated an early carbonation process as consequence of Li_2O high reactivity with CO_2 at room temperature [30]. Likewise, the MgO hygroscopic nature and its spontaneous carbonation at room temperature were also contemplated.

As expected, the vibration band of the carbonates ion was observed within the spectra for the samples treated at 40 °C–50% RH and 60 °C–70% RH. However, it is interestingly to observe the same vibration band within spectra for the same samples after being thermally decomposed, suggesting some remanence of carbonate species on their surface, being attributed to the Li_2CO_3 compound.

3.4.4. Thermogravimetric analysis

Fig. 10 displays the TGA-DTG experiments performed on samples with the highest weight increment after kinetic isothermal experiments

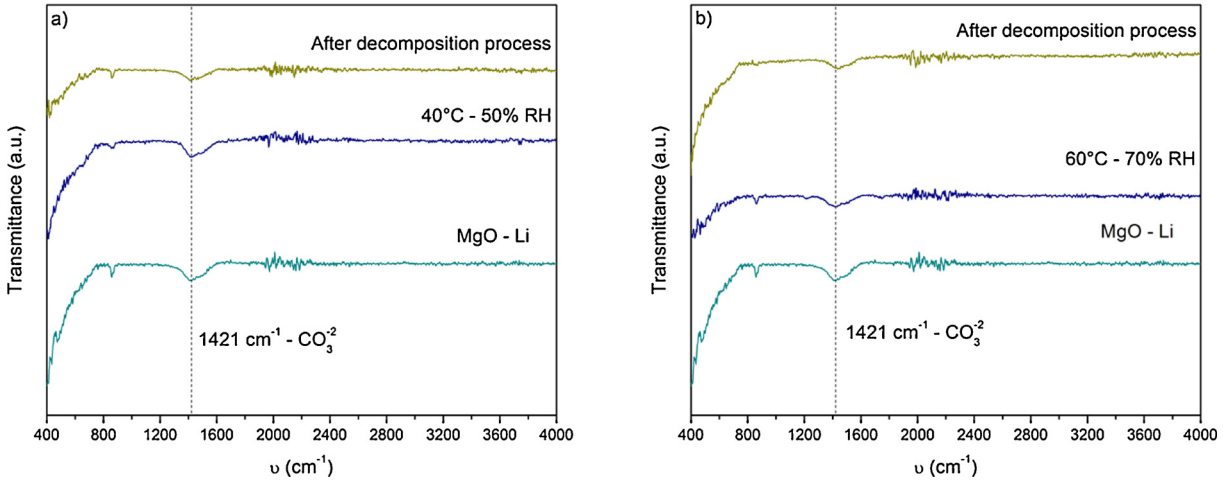

Fig. 9. FTIR spectra for samples treated at (a) 40 °C–50% RH and (b) 60 °C–70% RH.

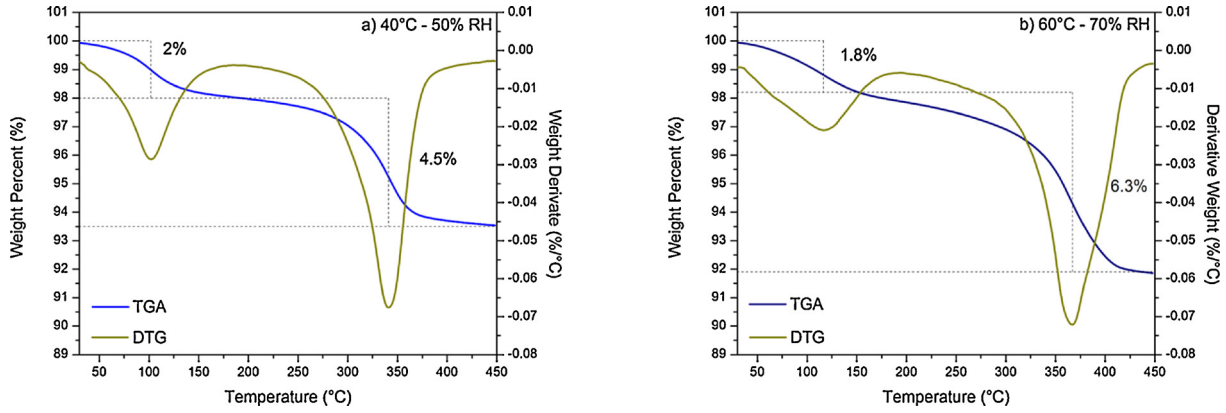

Fig. 10. TGA-DTG curves for samples treated at (a) 40 °C–50% RH and (b) 60 °C–70% RH, respectively.

(40 °C–50% RH and 60 °C–70% RH). In these thermograms, a weight loss attributed to dehydration process from 25 to 200 °C was clearly observed. Within this temperature range, the difference between the amount of water adsorbed for 40 °C–50% RH (~2wt%) and 60 °C–70% RH (~1.8wt%), was not significant. Therefore, the impregnation of Li on the surface of open-cell Mg foams did not have a significant effect on the total amount of adsorbed water.

A second drop in weight was observed between 250 and 375 °C, being attributed to the decomposition process of $MgCO_3$ [46]. In comparison to the total weight increments after the kinetic isothermal experiments for samples treated at 40 °C–50% RH and 60 °C–70% RH, their registered weight loss after thermal decomposition process was below 1%. Therefore, these results suggested the feasible presence of lithium carbonates, since it was not possible to deny the significant improvement on the H_2O–CO_2 chemisorption capacity after the addition of Li. In addition, it cannot be argued that lithium carbonates must be completely decomposed within the temperature range from 250 to 375 °C. FTIR results and the melting point of Li_2CO_3 (710 °C) support these statements, as the IR spectra displayed the vibration band of the carbonate ion, after the thermal decomposition process. However, it is not possible to detail the total amount of CO_2 adsorbed (mmol/g) since the Li_2CO_3 remains on the surface. Overall, these results confirm a notable improvement in the CO_2 capture capacity on the surface of open-cell Mg foams after being impregnated with Li.

4. Conclusions

The addition of Li on the surface of an open-cell Mg foam did modify the textural properties, and therefore the CO_2 capture capacity. Regarding textural properties, it has been proved that the addition of Li and the subsequent oxidization stage have a noteworthy effect on the specific surface area. Characterization by means of N_2 adsorption-desorption isothermal experiments showed a considerable increment from 5.5 to 16.7 m^2/g. This can be considered important, since the open-cell Mg foams fabricated in the present work were not prepare by powder metallurgy. Furthermore, the dynamic and kinetic isothermal experiments clearly showed an important enhancement on the CO_2 capture capacity performed by open-cell Mg foams after being impregnated with Li. These results support the feasible utilization of open-cellular materials as structured CO_2 captors with the aim to alleviate the current environmental issues.

Acknowledgements

This work was financially supported by UNAM-DGAPA-PAPPIT (No. IN101016). M. Velasco-Castro would like to acknowledge the financial support from the National Council for Science and Technology (CONACYT) of Mexico for the Scholarship 583061. A. Tejada-Cruz, J. Romero-Ibarra, F. García-López, A. López-Vivas, J. M. García-León, R. Reyes-Ortiz, F. Silvar-Gómez, C. Ramos, O. Novelo-Peralta, C. Flores-Morales, E. Hernández-Mecinas and G. Lara-Rodríguez are also acknowledged for their technical support. *"Por mi raza hablará el espíritu"*.

References

[1] L.J. Gibson, M.F. Ashby, Cellular Solids Structure and Properties, 2nd ed., Cambridge University Press, 1999.
[2] T.W. Clyne, F. Simancik, Metal Matrix Composites and Metallic Foams, Wiley-VCH, 2000.
[3] J. Banhart, Manufacture, characterisation and application of celular metals and metal foams, Prog. Mater. Sci. 46 (2001) 559–632.
[4] H.-P. Degischer, B. Kriszt, Handbook of Cellular Metals: Production, Processing, Applications, Wiley-VCH, 2002.
[5] R. Goodall, A. Mortensen, Porous Metals, in Physical Metallurgy, Elsevier Inc., 2014.
[6] I.A. Figueroa, et al., Development of pure Mg open-cell foams as structured CO_2 captor, Thermochim. Acta 621 (2015) 74–80.
[7] C.E. Wen, et al., Processing of biocompatible porous Ti and Mg, Scr. Mater. 45 (2001) 1147–1153.
[8] J. Trinidad, et al., Processing of magnesium porous structures by infiltration casting for biomedical applications, Adv. Eng. Mater. 16 (2) (2014) 241–247.
[9] IPCC, Climate Change: 2007 Synthesis Report, (2008).
[10] S. Choi, J.H. Drese, C.W. Jones, Adsorbent materials for carbon dioxide capture from large anthropogenic point sources, ChemSusChem 2 (2009) 796–854.
[11] H. Pfeiffer, Advances on alkaline ceramics as possible CO_2 captors, in advances in CO_2 conversion and utilization, Am. Chem. Soc. (2010) 233–253.
[12] D.M. D'Alessandro, B. Smit, J.R. Long, Carbon dioxide capture: prospects for new materials, Angew. Chem. Int. Ed. 49 (2010) 2–27.
[13] Q. Wang, et al., CO_2 capture by solid adsorbents and their applications: current status and new trends, Energy Environ. Sci. 4 (2011) 42–55.
[14] S. Wang, et al., Recent advances in capture of carbon dioxide using alkali-metal-based oxides, Energy Environ. Sci. 4 (2011) 3805–3819.
[15] K. Sumida, et al., Carbon dioxide capture in metal-organic frameworks, Chem. Rev. 112 (2012) 724–781.
[16] M. Pera-Titus, Porous inorganic membranes for CO_2 capture: present and prospects, Chem. Rev. 114 (2014) 1413–1492.
[17] M.Z. Memon, et al., Alkali metal CO_2 sorbents and the resulting metal carbonates: potential for process intensification of sorption-enhanced steam reforming, Environ. Sci. Technol. 51 (1) (2017) 12–27.
[18] J. Ortiz-Landeros, et al., Analysis and perspectives concerning CO_2 chemisorption on lithium ceramics using thermal analysis, J. Therm. Anal. Calorim. 108 (2012) 647–655.
[19] T. Ávalos-Rendón, V.H. Lara, H. Pfeiffer, CO_2 Chemisorption and, Cyclability analyses of lithium aluminate polymorphs (α- and β-Li_5AlO_4), Ind. Eng. Chem. Res. 51 (2012) 2622–2630.
[20] T.L. Ávalos-Rendón, H. Pfeiffer, High CO_2 chemisorption in α-Li_5AlO_4 at low temperatures (30–80 °C): effect of the water vapor addition, Energy Fuels 26 (2012) 3110–3114.
[21] H.A. Lara-García, et al., Water steam effect during high CO_2 chemisorption in lithium cuprate (Li_2CuO_2) at moderate temperatures: experimental and theoretical evidence, RSC Adv. 5 (2015) 34157–34165.
[22] J.F. Gomez-García, H. Pfeiffer, Structural and CO_2 capture analyses of the $Li_{1+x}FeO_2$ ($0 < x < 0.3$) system: effect of different physicochemical conditions, RSC Adv. 6 (2016) 112040–112049.
[23] B. Alcántar-Vázquez, et al., Analysis of the CO_2-H_2O chemisorption in lithium silicates at low temperatures (30–80 °C), Ind. Eng. Chem. Res. 54 (2015) 6884–6892.
[24] L. Martínez-dlCruz, H. Pfeiffer, Toward understanding the effect of water sorption on lithium zirconate (Li_2ZrO_3) during its carbonation process at low temeratures, J. Phys. Chem. C 114 (2010) 9453–9458.

[25] D. Iruretagoyena, et al., Influence of alkali metals (Na, K, and Cs) on CO_2 adsorption by layered double oxides supported on graphene oxide, Ind. Eng. Chem. Res. 54 (2015) 11610–11618.
[26] N.N.A.H. Meis, J.H. Bitter, K.P. de Jong, On the influence and role of alkali metals on supported and unsupported activated hydrotalcites for CO_2 sorption, Ind. Eng. Chem. Res. 49 (2010) 8086–8093.
[27] T. Harada, et al., Alkali metal nitrate-promoted high-capacity MgO adsorbents for regenerable CO_2 capture at moderate temperatures, Chem. Mater. 27 (2015) 1943–1949.
[28] E. Ghali, R.W. Revie, Corrosion Resistance of Aluminum and Magnesium Alloys: Understanding, Performance and Testing, John Wiley & Sons Inc., 2010.
[29] W.A. Ferrando, Review of corrosion and corrosion control of magnesium alloys and composites, J. Mater. Eng. 11 (4) (1989) 299–313.
[30] H.A. Mosqueda, et al., Chemical sorption of carbon dioxide (CO_2) on lithium oxide (Li_2O), Chem. Mater. 18 (2006) 2307–2310.
[31] C. Trionfetti, et al., Formation of high surface area Li/MgO-efficient catalyst for the oxidative dehydrogenation/cracking of propane, Appl. Catal. A Gen. 310 (2006) 105–113.
[32] C. Trionfetti, et al., Presence of lithium ions in MgO lattices: surface characterization by infrared spectroscopy and reactivity towards oxidative conversion of propane, Langmuir 24 (2008) 8220–8228.
[33] M. de Graef, M.E. McHenry, Structure of Materials: An Introduction to Crystallography, Diffraction and Symmetry, 2nd ed., Cambridge University Press, 2012.
[34] J.H. Nordlien, S. Ono, N. Masuko, Morphology and structure of oxide films formed on magnesium by exposure to air and water, J. Electrochem. Soc. 142 (10) (1995) 3320–3322.
[35] N. Hara, et al., Formation and breakdown of surface films on magnesium and its alloys in aqueous solutions, Corros. Sci. 49 (2007) 166–175.
[36] M. Santamaria, et al., Initial suface film on magnesium metal: a characterization by X-ray photoelectron spectroscopy (XPS) and photocurrent spectroscopy (PCS), Electrochim. Acta 53 (2007) 1314–1324.
[37] Y. Song, et al., Investigation of surface oxide film on magnesium lithim alloy, J. Alloys Compd. 484 (2009) 585–590.
[38] J.B. Condon, Surface Area and Porosity Determination by Physisorption: Measurements and Theory, Elsevier B.V., 2006.
[39] S. Lowell, et al., Characterization of Porous Solids and Powders: Suface Area, Pore Size and Density, Springer Science + Business Media, New York, 2004.
[40] R. Rodríguez-Mosqueda, H. Pfeiffer, High CO_2 capture in sodium metasilicate (Na_2SiO_3) at low temperatures (30–60 °C) through the CO_2-H_2O chemisorption process, J. Phys. Chem. C 117 (2013) 13452–13461.
[41] L. Martínez-dlCruz, H. Pfeiffer, Microstructural thermal evolution of the Na_2CO_3 phase produced during a Na_2ZrO_3-CO_2 chemisorption process, J. Phys. Chem. C 116 (2012) 9675–9680.
[42] D.A. Torres-Rodríguez, H. Pfeiffer, Thermokinetic analysis of the MgO surface carbonation process in the presence of water vapor, Thermochim. Acta 516 (2011) 74–78.
[43] R.V. Siriwardane, R.W. Stevens Jr., Novel regenerable magnesium hydroxide sorbents for CO_2 capture at warm gas temperatures, Ind. Eng. Chem. Res. 48 (2009) 2135–2141.
[44] K. Nakamoto, Infrared and Raman Spectra of Inorganic and Coordination Compounds Part B: Applications in Coordination, Organometallic and Bioinorganic Chemistry, 6th ed., John Wiley & Sons, Inc., 2009.
[45] F.A. Miller, C.H. Wilkins, Infrared spectra and characteristic frequencies of inorganic ions: their use in qualitative analysis, Anal. Chem. 24 (8) (1952) 1253–1294.
[46] J.C. Fisher, R.V. Siriwardane, $Mg(OH)_2$ for CO_2 capture from high-pressure, moderate-temperature gas streams, Energy Fuels 28 (2014) 5936–5941.